Retinal Pigment Epithelial Cells Control Early Mycobacterium tuberculosis Infection via Interferon Signaling

Nora, R.L.; Walburg, K.V.; Hagen, P.M. van; Swagemakers, S.M.A.; Spek, P.J. van der; Quinten, E.; ... ; Haks, M.C.

Retinal Pigment Epithelial Cells Control Early *Mycobacterium tuberculosis* Infection via Interferon Signaling

Rina La Distia Nora,[1,2] Kimberley V. Walburg,[3] P. Martin van Hagen,[1,4] Sigrid M. A. Swagemakers,[5] Peter J. van der Spek,[5] Edwin Quinten,[3] Mirjam van Velthoven,[6] Tom H. M. Ottenhoff,[3] Willem A. Dik,[1,7] and Mariëlle C. Haks[3]

[1]Department of Immunology, Erasmus Medical Center, Rotterdam, The Netherlands
[2]Department of Ophthalmology, University of Indonesia and Cipto Mangunkusumo Hospital Kirana, Jakarta, Indonesia
[3]Department of Infectious Diseases, Leiden University Medical Center, Leiden, The Netherlands
[4]Department of Internal Medicine, Section Clinical Immunology, Erasmus Medical Center, Rotterdam, The Netherlands
[5]Department of Bioinformatics, Erasmus Medical Center, Rotterdam, The Netherlands
[6]Rotterdam Eye Hospital, Rotterdam, The Netherlands
[7]Laboratory Medical Immunology, Erasmus Medical Center, Rotterdam, The Netherlands

Correspondence: P. Martin van Hagen, Erasmus Medical Center, Department of Immunology, Wytemaweg 80, 3015 CN Rotterdam, The Netherlands; p.m.vanhagen@erasmusmc.nl.

RLDN and KVW contributed equally to the work presented here and should therefore be regarded as equivalent authors.

THMO, WAD, and MCH contributed equally to the work presented here and should therefore be regarded as equivalent authors.

Submitted: October 28, 2017
Accepted: January 21, 2018

Citation: La Distia Nora R, Walburg KV, van Hagen PM, et al. Retinal pigment epithelial cells control early *Mycobacterium tuberculosis* infection via interferon signaling. *Invest Ophthalmol Vis Sci*. 2018;59:1384–1395. https://doi.org/10.1167/iovs.17-23246

Purpose. *Mycobacterium tuberculosis* (*Mtb*) bacilli have been found in retinal pigment epithelial (RPE) cells from uveitis patients without signs of systemic tuberculosis (TB) infection. RPE cells are important for ocular immune privilege and uveitis development.

Methods. To address a potential role for *Mtb*-infected RPE cells in the development of uveitis, we delineated the response to *Mtb* infection in human RPE cells and primary human macrophages, the main target cell of *Mtb*. Primary human RPE cells, the human RPE cell line ARPE-19, and monocyte-derived proinflammatory M1 and anti-inflammatory M2 macrophages were infected with DsRed-expressing *Mtb* strain H37Rv. Infection rates and clearance were addressed along with RNA sequencing analysis, a confirmation analysis by dual-color reverse-transcriptase multiplex ligation-dependent probe amplification (dcRT-MLPA) and cytokine secretion.

Results. RPE cells robustly controlled intracellular outgrowth of *Mtb* early after infection. The response in RPE cells to control *Mtb* survival was dominated by interferon (IFN) signaling and further characterized by prominent regulation of cell death/survival–associated genes and low-level production of Th1-associated cytokines. In contrast, macrophages engaged a plethora of responses including IFN signaling and communication between innate and adaptive immune cells to induce granuloma formation.

Conclusions. Together, our data demonstrate that RPE cells display a strong response to *Mtb* infection that appears, however, incomplete in comparison to the macrophage response to *Mtb*. The RPE response might reflect a balance between mechanisms aimed at *Mtb* eradication and mechanisms that limit retinal inflammation.

Keywords: tuberculosis, retinal pigment epithelial (RPE) cells, macrophages, IFN signaling, immune profiling

Tuberculosis (TB) is a global health issue with one-fourth of the world population being latently infected. It is the world's leading cause of death from infectious diseases as 1.8 million people died from TB in 2015 alone.[1] TB primarily infects (alveolar) macrophages in the lungs, and its causative agent *Mycobacterium tuberculosis* (*Mtb*) spreads via airborne droplets from active pulmonary TB patients to other susceptible individuals.[2] The infected host first initiates an innate immune response to limit *Mtb* infection, which is followed by an adaptive immune response and formation of caseating granulomas.[3,4] However, *Mtb* exhibits immune evasion strategies to survive and replicate within macrophages and disseminate from the primary focus throughout the body via blood and the lymphatic system.[5]

Mtb can also infect other cell types, including epithelial cells, endothelial cells, fibroblasts, adipocytes, and neuronal cells.[5,6] Persistence of *Mtb* in such cell types distant from the lungs may constitute reservoirs that can reactivate TB disease, resulting in extrapulmonary TB.[5] Notably, several histopathologic studies have described uveitis cases that, due to a lack of systemic symptoms, were not suspected to be active TB cases but obviously did contain *Mtb* in the retinal pigment epithelium (RPE).[7,8] Although very few *Mtb* bacilli were detected in RPE cells, necrosis or severe granulomatous inflammation around the RPE cells was observed, suggesting a role for *Mtb*-infected RPE cells in driving these responses. Therefore, knowledge of the host–pathogen interaction between *Mtb* and RPE cells and the immune responses induced by *Mtb*-infected RPE cells will provide critical pathophysiological insights into how *Mtb* can cause uveitis. Importantly, RPE cells have been described to phagocytose *Mtb,* resulting in increased expression of Toll-like receptor (TLR)2 and TLR4, which are major pattern recognition

receptors (PRRs) for sensing *Mtb*.[9,10] Moreover, chemical inhibition of TLR2 and TLR4 on RPE cells reduced the number of intracellular *Mtb* bacilli, suggesting an essential role for these receptors in phagocytosis of *Mtb* by RPE cells.[9] Yet, limited data are available on the response of RPE cells to *Mtb* infection and how this response compares to the response elicited in human macrophages, the predominant target cell of *Mtb* in the lungs.

In this study, we infected primary human RPE cells (OZR1), the human RPE cell line ARPE-19, and primary human monocyte-derived proinflammatory (M1) and anti-inflammatory (M2) macrophages with *Mtb* to investigate the host–pathogen interaction between these cells and *Mtb*, as well as the host response induced in these cells to infection with *Mtb*. Transcriptomics and cytokine secretion data were analyzed to discover crucial signaling pathways/networks and biological effector functions regulated in *Mtb*-infected RPE cells and macrophage subtypes. Our findings suggest that while M2 cells have a plethora of responses, including IFN signaling, to control *Mtb* infection, RPE cells primarily depend on IFN signaling to control the early phases of *Mtb* infection successfully.

Materials and Methods

Cell Culture

Primary human RPE cells (OZR1)[11] and the human RPE cell line ARPE-19 (CRL-2302; American Type Culture Collection, Manassas, VA, USA) were maintained in Iscove's Modified Dulbecco's Medium (IMDM) supplemented with 10% fetal bovine serum (FBS; Greiner Bio-One, Alphen aan den Rijn, The Netherlands). For experiments, OZR1 cells were used between the 6th and 10th passages and ARPE-19 cells between the 25th and 39th passages.

Proinflammatory M1 and anti-inflammatory M2 macrophages were generated from monocytes isolated from whole blood of healthy donors by FICOLL gradient separation and CD14 MACS sorting (Miltenyi Biotec, Teterow, Germany) followed by differentiation for 6 days in the presence of either 5 ng/mL recombinant granulocyte-macrophage colony-stimulating factor (GM-CSF; Life Technologies, Bleiswijck, The Netherlands) or 50 ng/mL recombinant macrophage colony-stimulating factor (M-CSF; R&D Systems, Abingdon, UK), respectively, as previously reported.[12] Macrophages were maintained in Gibco Roswell Park Memorial Institute (RPMI) 1640 medium (Life Technologies) supplemented with 10% FBS (Greiner Bio-One), 100 U/mL penicillin, and 100 μg/mL streptomycin (Life Technologies).

Mycobacterial Culture

DsRed-expressing *Mtb* strain H37Rv was cultured in Difco Middlebrook 7H9 broth (Becton Dickinson, Breda, The Netherlands) supplemented with 10% albumin dextrose catalase (ADC; Becton Dickinson), 0.5% Tween-80 (Sigma-Aldrich Chemie B.V., Zwijndrecht, The Netherlands) and 50 μg/mL hygromycin B (Life Technologies). DsRed was expressed from expression plasmid pSMT3 and expression was under the control of the mycobacterial heat shock promoter Phsp60.[13]

Mycobacterial Infection

Mycobacterial cultures were diluted to pre-log phase density with appropriate antibiotics 1 day before infection (optical density at 600 nm [OD600] of 0.4). Immediately before infection, bacterial density was determined, and the bacterial suspension was diluted to 30×10^6 bacteria/mL in cell culture medium without antibiotics (multiplicity of infection [MOI] = 10). The accuracy of bacterial density was verified by colony-forming unit (CFU) assay. RPE cells, seeded 24 hours prior to infection at 30×10^4 cells/24 wells, were inoculated with 100 μL of the bacterial suspension, centrifuged (3 minutes, 129*g*), and incubated (60 minutes: 37°C, 5% CO_2). Plates were then washed with culture medium containing 30 μg/mL gentamicin sulfate (Lonza BioWhittaker, Basel, Switzerland) and incubated at 37°C and 5% CO_2 in medium containing 5 μg/mL gentamicin until readout by flow cytometry, confocal microscopy, or CFU assay as described previously.[14]

Confocal Microscopy

Cells (27×10^4 cells) were grown overnight on 35-mm glass bottom microwell dishes (MatTek Corporation, Ashland, MA, USA) and infected as described above. Samples were stained with Phalloidin-Alexa Fluor 488 (Life Technologies) in PBS to visualize F-actin. Samples were subsequently fixed for 30 minutes at room temperature with 4% paraformaldehyde (PFA), embedded in VectaShield with DAPI (Brunschwig Chemie, Amsterdam, The Netherlands). Microscopy slides were examined on a Leica TCS SP5 confocal microscope (Leica Microsystems B.V., Eindhoven, The Netherlands).

Phagocytosis

To quantify the phagocytic capacity of cells, fluorescent polystyrene particles 2 μm in diameter with carboxylate coating (Fluoresbrite YG Carboxylate Microspheres; Polyscience, Eppelheim, Germany) were used as described previously.[15] For details see Supplementary Materials.

RNA Isolation and Dual-Color Reverse-Transcriptase Multiplex Ligation-Dependent Probe Amplification (dcRT-MLPA)

RNA isolation and dcRT-MLPA were performed as described elsewhere.[16] For details see Supplementary Materials. Trace data were analyzed using GeneMapper software 5 package (Applied Biosystems, Warrington, UK). The areas of each assigned peak (in arbitrary units) were exported for further analysis in Microsoft Excel spreadsheet software (Microsoft Corp., Redmond, WA, USA). Data were normalized to *GAPDH*, and signals below the threshold value for noise cutoff in GeneMapper (Applied Biosystems, Warrington, UK) (Log2 transformed peak area 7.64) were assigned the threshold value for noise cutoff. Finally, the normalized data were Log2 transformed for statistical analysis.

RNA Sequencing and Pathway and Network Analysis

RNA sequencing was performed by ZF-Screens B.V. (Leiden, The Netherlands). For detail see Supplementary Materials. Differential gene expression results were analyzed using Partek (Partek Genomics Suite software, version 6.6; Partek, Inc., St. Louis, MO, USA), Ingenuity Pathway Analysis (IPA; QIAGEN, Redwood City, CA, USA), DAVID (open access Database for Annotation, Visualization, and Integrated Discovery; DAVID Bioinformatics Resources, Frederick, MD, USA), and Instem/OmniViz Treescape (version 6.1.13.0; Instem Scientific, Staffordshire, UK) software tools.

Cytokine, Chemokine, and Growth Factor Assay Analysis

Culture supernatants were analyzed using the Bio-Plex Pro Human Cytokine, Chemokine, and Growth Factor Assay

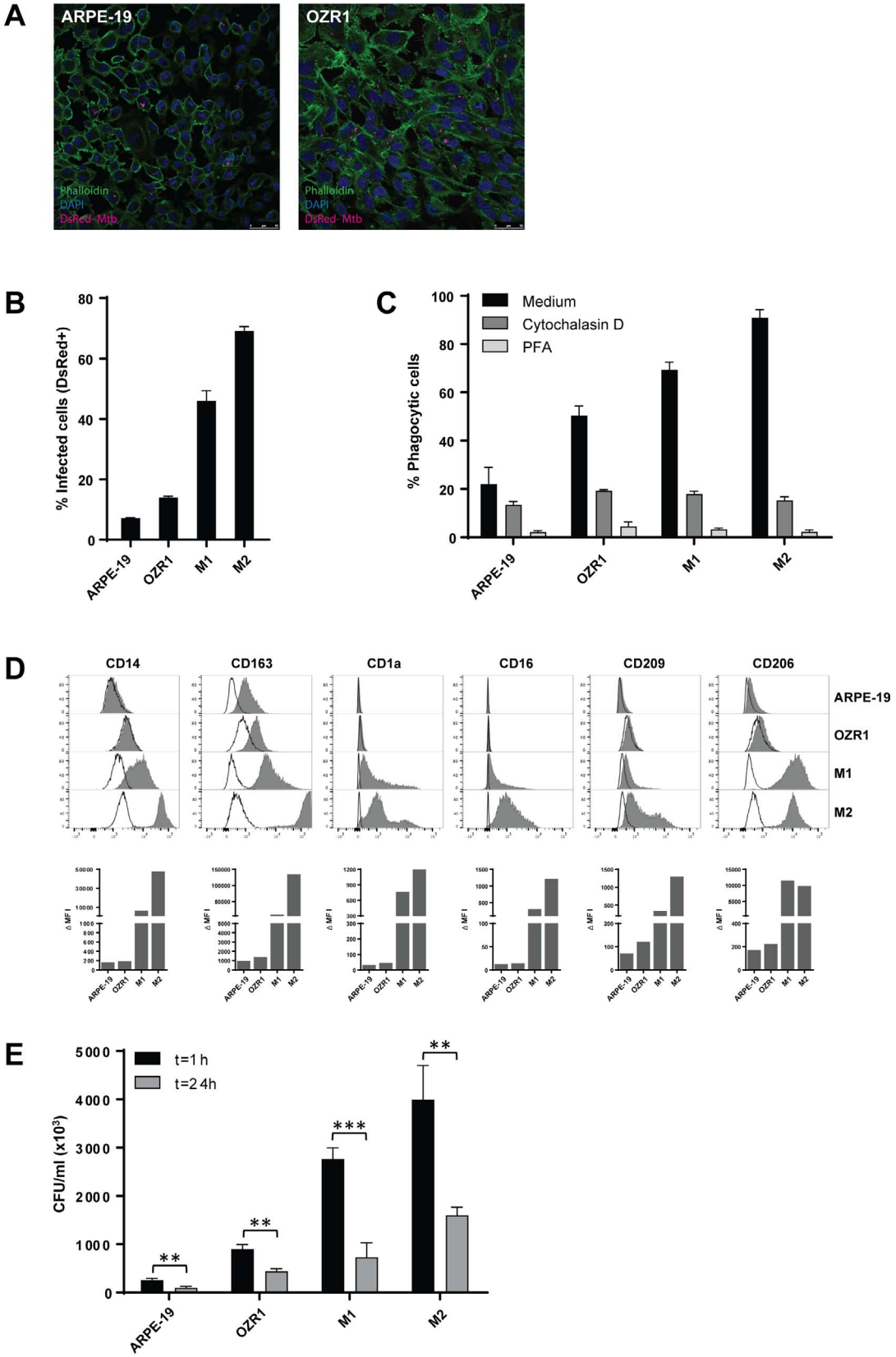

Figure 1. Both RPE and macrophage subsets infected with *Mtb* can control intracellular bacterial survival. (**A**) Confocal microscopy of RPE cells 24 hours after infection with DsRed-expressing *Mtb*. (**B**) Flow cytometric analysis of RPE cells (ARPE-19 and OZR1) and macrophage subsets (M1 and M2) 24 hours after infection with DsRed-expressing *Mtb*. Percentages of DsRed-positive events are indicated. A representative result of three experiments is shown. *Bars* display mean of triplicates ± standard deviation. (**C**) Percentage of phagocytic cells after trypan blue quenching was determined by confocal microscopy. Percentages of phagocytic cells were determined in each cell type, without (*black bars*) or with preincubation

of phagocytosis inhibitors, 5 μM Cytochalasin D (*dark gray bars*) or 4% paraformaldehyde (PFA) (*light gray bars*). (**D**) Expression of cell surface markers associated with phagocytosis was determined by flow cytometry. Δ Mean fluorescence intensity (MFI) (*bottom*) was calculated between antigen-specific staining (*gray histograms*) and isotype control staining (*white histograms*) (*top*). (**E**) Colony-forming unit assays were performed at $t = 1$ hour (end of the infection period) and $t = 24$ hours after infection with *Mtb*. A representative result of three experiments is shown. *Bars* display mean of triplicates ± standard deviation. Statistical significance was tested using a Student's *t*-test. $^{**}P < 0.01$, $^{***}P < 0.001$.

(BioRad, Hercules, CA, USA) for IL-1β, IL-1Ra, IL-2, IL-4, IL-5, IL-6, IL-7, IL-8/CXCL8, IL-9, IL-10, IL-12 (p70), IL-13, IL-15, IL-17, bFGF, eotaxin, G-CSF, GM-CSF, IFNγ, interferon gamma-induced protein (IP)-10/CXCL10, monocyte chemotactic protein (MCP)-1/CCL2, macrophage inflammatory protein (MIP)-1α/CCL3, MIP-1β/CCL4, PDGF-BB, regulated on activation, normal T cell expressed and secreted (RANTES/CCL5), TNFα, and VEGFA. The assay was performed according to the manufacturer's instructions.

Statistical Analysis

Mtb bacterial load, cytokine/chemokine/growth factors, and dcRT-MLPA data were analyzed for statistical significance using a 2-tailed unpaired Student's *t*-test. A P value ≤ 0.05 was considered significant. For the RNA sequencing data set, P values were adjusted for multiple testing using the Benjamini-Hochberg procedure, which controls the false discovery rate (FDR). The statistical computation was performed using GraphPad 7 (La Jolla, CA, USA) and SPSS 22 software (IBM Corp, Armonk, NY, USA).

Results

Macrophages and RPE Cells Infected With *Mtb* Control Intracellular Bacterial Growth

To validate previous findings that *Mtb* can be phagocytosed by RPE cells,[9] ARPE-19 and OZR1 cells were infected with DsRed-expressing *Mtb* strain H37Rv. Confocal microscopy and Z-scan analyses clearly revealed intracellular localization of *Mtb* bacilli, confirming that *Mtb* can infect RPE cells (Fig. 1A). The percentage of *Mtb*-infected cells was markedly higher in proinflammatory M1 and anti-inflammatory M2 macrophages than in the RPE cells ARPE-19 and OZR1 (Fig. 1B). *Mtb* requires active phagocytosis by host cells, and the differences in infection rate between macrophage subsets and RPE cells indeed correlated with their phagocytic capacity (Fig. 1C) and expression of phagocytosis-associated cell surface markers (Fig. 1D). To address whether RPE cells, like macrophages, control *Mtb* infection, intracellular bacterial loads were determined immediately after infection with *Mtb* ($t = 1$ hour) and compared to intracellular bacterial load 24 hours after infection (Fig. 1E). Comparable with M1 and M2 macrophages, a significant reduction in CFUs was observed in ARPE-19 and OZR1 cells over time, indicating that RPE cells are able to reduce the intracellular survival of *Mtb* and control the mycobacterial infection. However, OZR1 cells showed more *Mtb* load to begin with ($t = 1$ hour) than ARPE-19 cells, which is in line with the higher proportion of phagocytic cells observed for OZR1 in comparison to ARPE-19 (Fig. 1C).

Characterization of the Host Response at the Transcriptomic Level in RPE Cells and Macrophages Infected With *Mtb*

Next, we characterized the host response induced in RPE cells and macrophages upon *Mtb* infection to (1) identify crucial host signaling pathways and networks regulating intracellular bacterial survival and (2) address whether similar regulatory networks are operational in RPE cells and macrophages to control outgrowth of *Mtb*. Global transcriptional changes induced in primary human RPE cells OZR1 and human anti-inflammatory M2 macrophages following *Mtb* infection were determined in triplicate samples by RNA sequencing. M2 macrophages were selected for RNA sequencing since they share many characteristics with alveolar macrophages, the predominant target of *Mtb* in vivo in the human lung. Principal component analysis (PCA) analysis indicated profound differences between the overall gene expression patterns of *Mtb*-infected cells and their uninfected counterparts, with the largest changes found between infected and uninfected M2 macrophages (Fig. 2A). This could reflect a stronger regulation of commonly altered genes in M2 compared to OZR1 cells and/or regulation of a larger and more diverse gene repertoire in macrophages compared to RPE cells.

To first identify individual genes that were differentially expressed following *Mtb* infection, cutoff values for fold change >1.5 and P value ≤0.01 were applied to the data set. A total of 390 and 1638 genes were differentially expressed in *Mtb*-infected OZR1 and M2 cells compared to their uninfected controls, respectively, of which 130 genes were commonly regulated by OZR1 and M2 cells in response to *Mtb* infection (Fig. 2B; Supplementary Table S1). Notably, not only does the host response to *Mtb* infection in M2 macrophages involve the regulation of an extended set of genes compared to OZR1 cells, but the magnitude of the response also appears superior in M2 cells compared to OZR1 as indicated by a larger overall fold induction of regulated genes (Fig. 2C).

Identification of Signaling Pathways and Networks Regulated in RPE Cells and Macrophages Upon Infection With *Mtb*

Next, genes that were found to be differentially expressed in OZR1 and M2 cells following *Mtb* infection were fed into Ingenuity Pathway Analysis to identify critical signaling pathways and networks involved in the host response of RPE cells and macrophages to control intracellular survival of *Mtb*. Hierarchical clustering of the top 25 canonical pathways indicated that the host response of human macrophages upon *Mtb* infection involved a broader spectrum of signaling pathways than primary human RPE cells, as the host response in RPE cells was primarily dominated by IFN signaling (Fig. 3). A detailed analysis of the signaling pathways commonly or exclusively regulated by M2 and OZR1 cells is shown in Supplementary Table S2 and Supplementary Figure S1. A key canonical pathway regulated by both M2 and OZR1 cells in response to infection was IFN signaling (Fig. 3, Supplementary Fig. S1). Of the differentially expressed genes annotated within this canonical pathway, 10 genes were shared between M2 and OZR1, while RPE cells differentially regulated 8 additional IFN-inducible genes and M2 cells regulated 2 additional IFN-inducible genes (Fig. 4). More importantly, the host response of both M2 macrophages and OZR1 cells involved type I as well as type II IFN signaling genes. Network analysis corroborated a central role for IFN signaling in the host response of both OZR1 and M2

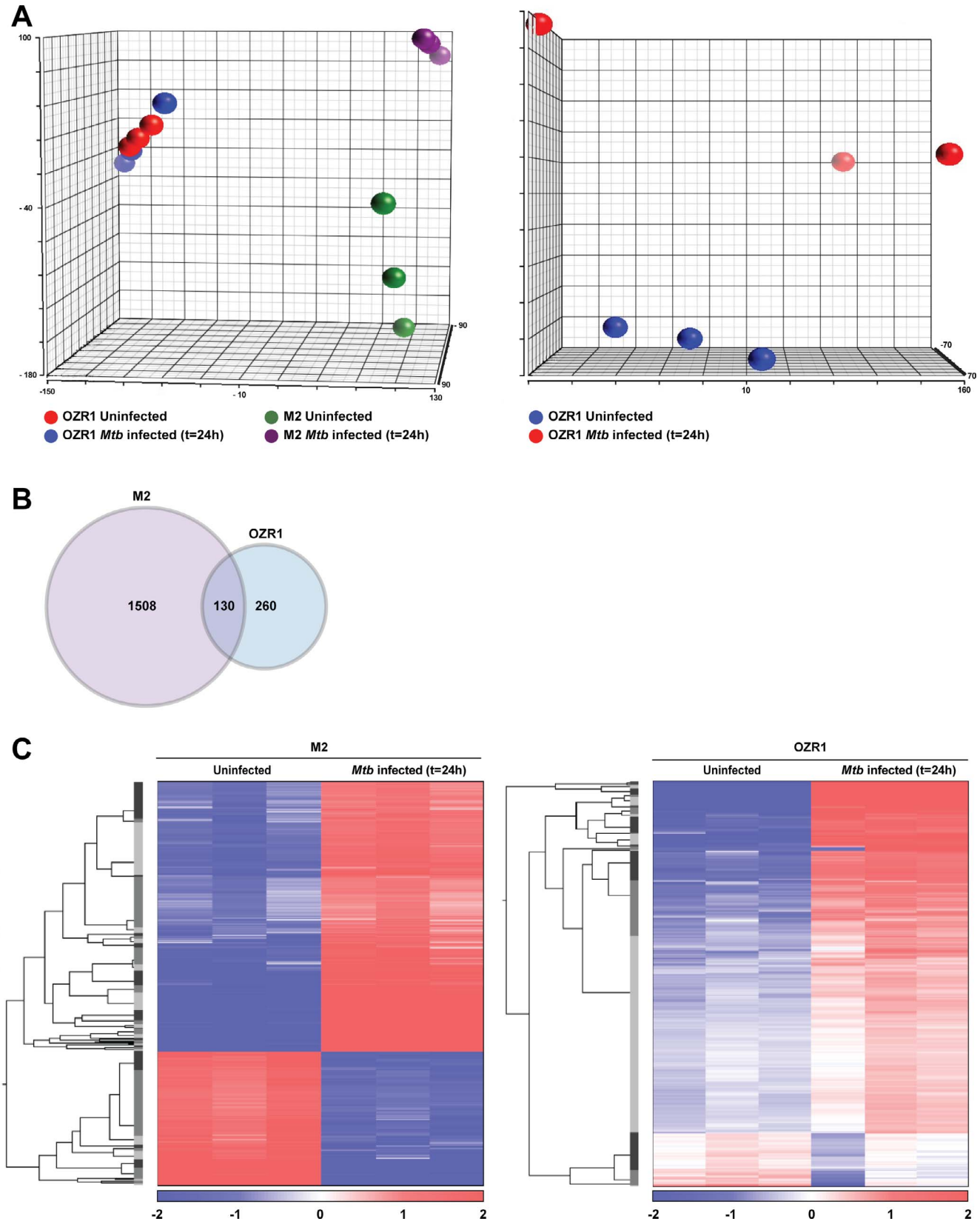

FIGURE 2. Characterization of the host response at the transcriptomic level in RPE cells and macrophages infected with *Mtb*. (**A**) PCA analysis of the overall gene expression profiles of uninfected and *Mtb*-infected ($t = 24$ hours) OZR1 and M2 macrophages. *Blue* and *red spheres* represent triplicate samples of uninfected and *Mtb*-infected OZR1 cells, whereas *green* and *purple spheres* represent triplicate samples of uninfected and *Mtb*-infected M2 macrophages, respectively. (**B**) Venn diagram of the number of differentially expressed genes (fold change > 1.5; P value ≤ 0.01) in *Mtb*-infected OZR1 and M2 macrophages compared to their uninfected controls. (**C**) OmniViz Treescape is displaying hierarchical clustering of the differentially

expressed transcripts identified in uninfected versus *Mtb*-infected M2 (*left*) and uninfected versus *Mtb*-infected OZR1 (*right*). *Red* indicates increased gene expression levels compared to the geometric mean; *blue* indicates decreased gene expression levels compared to the geometric mean. The color intensity correlates with the magnitude of the calculated fold change.

cells (Fig. 5). In addition, OZR1 cells selectively induced a cluster of *TRAIL* and *PARP* genes, belonging to a family of proteins mainly involved in DNA repair and programmed cell death, while M2 macrophages specifically regulated a cluster of ubiquitin-specific peptidases (*USP*) and a cluster of inflammasome-associated genes (Fig. 5, Supplementary Fig. S2).

Validation of the *Mtb*-Induced IFN Response Signature Using a Focused Gene Expression Profiling Platform

To validate independently the identified IFN response signature in OZR1 cells and M2 macrophages following *Mtb* infection and to investigate whether the identification of the IFN response signature can be confirmed in ARPE-19 cells and M1 macrophages upon *Mtb* infection, dcRT-MLPA was performed. This approach confirmed the IFN response signature in OZR1 and M2 cells in independent infection experiments (Supplementary Fig. S3). More importantly, the *Mtb*-induced IFN response signature was also confirmed in ARPE-19 cells, suggesting that the observed host response in OZR1 cells dominated by IFN signaling is a more general phenomenon in RPE cells. Interestingly, although macrophages displayed higher basal levels of IFN-inducible genes and a larger induction of expression of these transcripts following *Mtb* infection than RPE cells, the response kinetics to infection were significantly faster in RPE cells. Many IFN-inducible genes already reached maximum expression levels in RPE cells 1 hour after *Mtb* infection, while in macrophages the expression levels of most IFN-inducible genes were still comparable to baseline levels 1 hour after infection and were found elevated only at 24 hours after infection (Supplementary Fig. S3).

Characterization of the Host Response at the Protein Secretion Level in RPE Cells and Macrophages Infected With *Mtb*

Similar to the transcriptomic response, macrophages also secreted quantitatively and qualitatively more cytokines/chemokines/growth factors than RPE cells after *Mtb* infection (Fig. 6). Both OZR1 and ARPE-19 cells displayed a significantly enhanced secretion of IL-6, IL-8, and MCP-1 upon *Mtb* infection while OZR1 also displayed enhanced secretion of IFNγ, VEGFA, IL-12, IP10, TNFα, and RANTES. In both M1 and M2 macrophages MCP-1 secretion significantly decreased upon *Mtb* infection, while secretion of the other measured cytokines/chemokines/growth factors increased, except IL-5 and IL-13 (undetectable before and after infection). Interestingly, the protein secretion profiles of M1 and M2 were highly similar, and both macrophage subsets strongly induced secretion of MIP-1α, MIP-1β, and RANTES to absolute levels that profoundly surpassed the levels observed in RPE cells

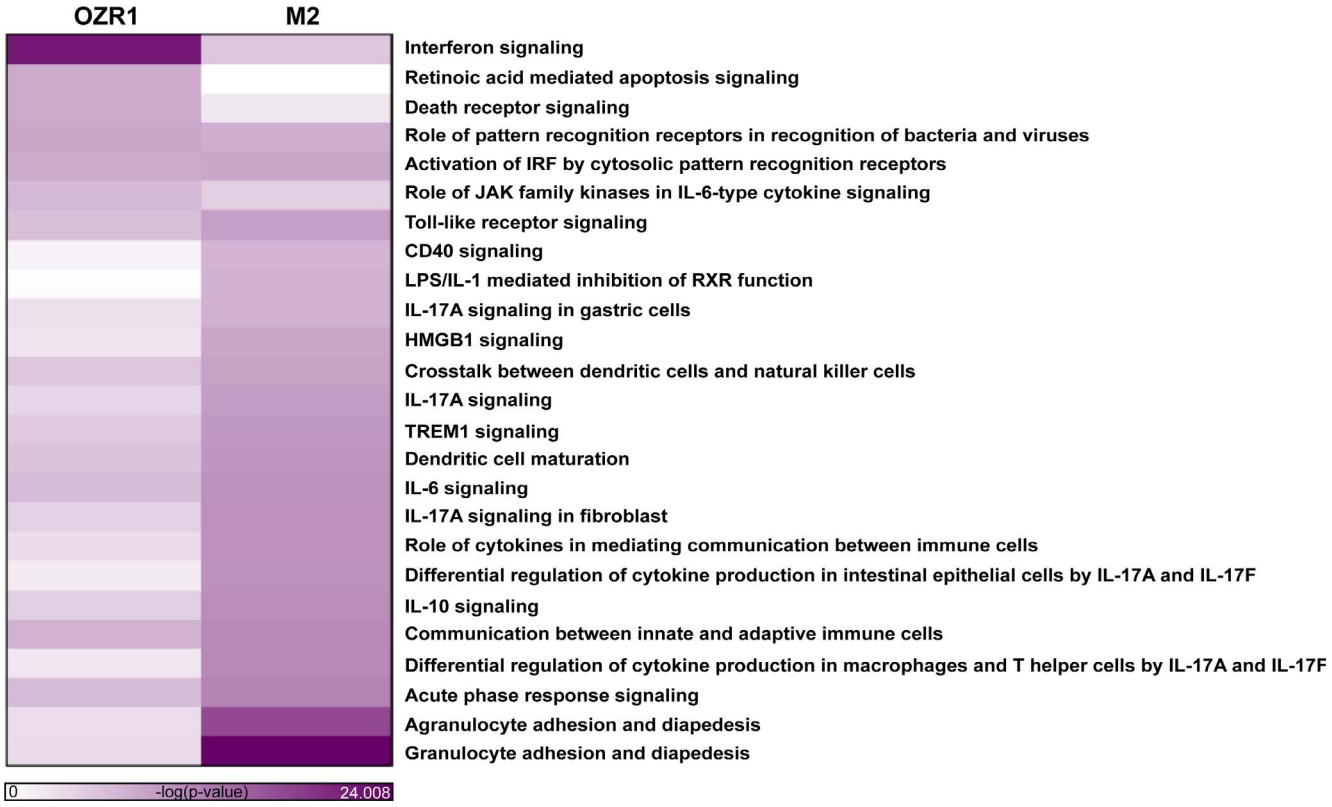

FIGURE 3. Identification of signaling pathways and networks regulated in RPE cells and macrophages upon infection with *Mtb*. Hierarchical clustering of the top 25 canonical pathways that were regulated with statistical significance in OZR1 and M2 cells following infection with *Mtb* ($t =$ 24 hours). The color coding of the map corresponds to the –log(*P* value) of each canonical pathway.

Investigative Ophthalmology & Visual Science

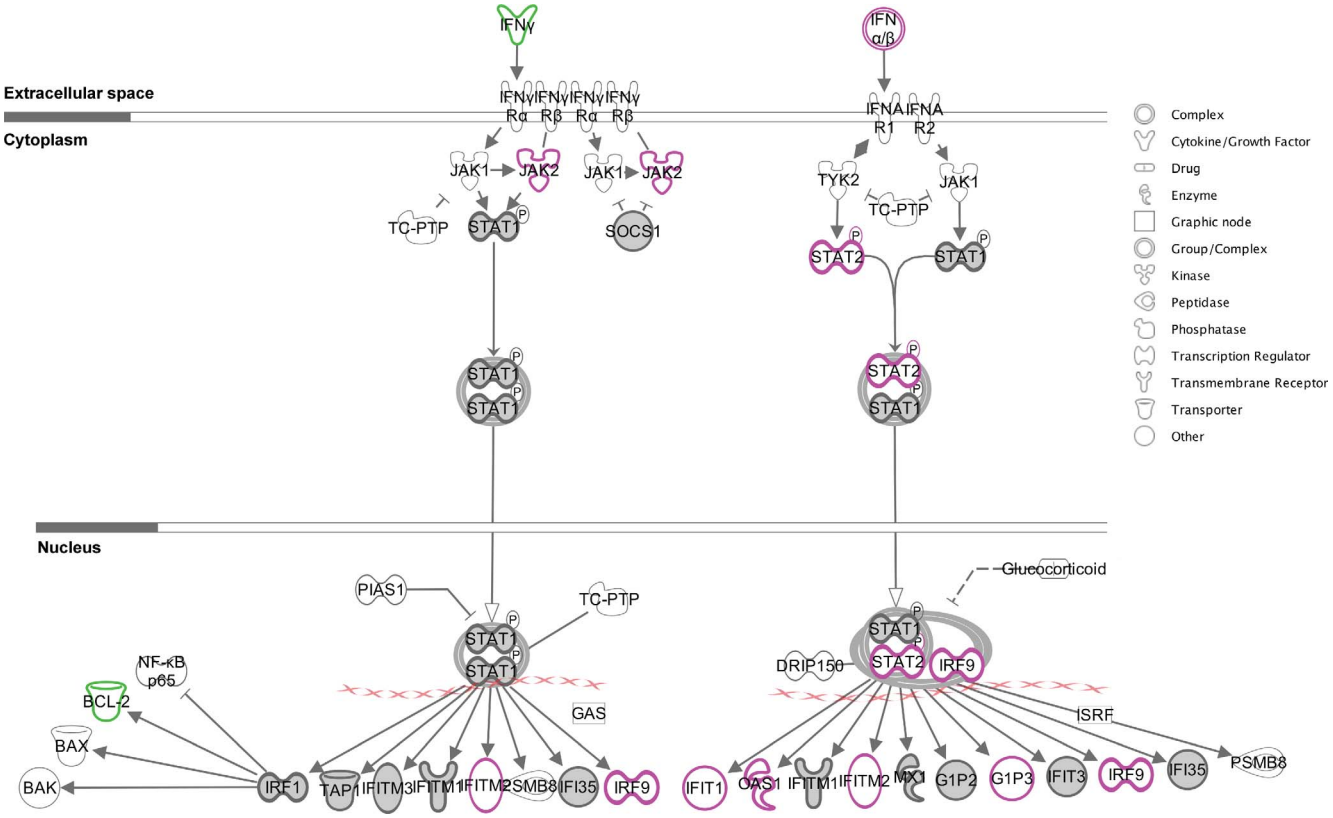

FIGURE 4. Both type I and II IFN signaling pathways are involved in the host response of RPE cells and macrophages against *Mtb*. Interferon signaling canonical pathway (Ingenuity Pathway Analysis). *Symbols* represent gene function. Indicated are genes that were differentially expressed in both OZR1 and M2 (*gray*) or solely regulated by OZR1 (*pink*) or M2 (*green*) in response to infection with *Mtb* ($t = 24$ hours).

(Supplementary Table S3). Together, these data suggest that while RPE cells focus their host response on eradicating *Mtb* through a response dominated by IFN signaling, macrophages upregulate in addition to IFN response–associated transcripts specifically the production of chemokines and cytokines involved in the granulomatous response by recruiting other macrophages and immune cells to the site of infection.

DISCUSSION

We demonstrated that *Mtb* could infect human RPE cells, although with a lower efficiency than human primary macrophages, and that RPE cells, like macrophages, control the intracellular survival of *Mtb* bacilli. Furthermore, we uncovered that the regulatory host response to *Mtb* in both proinflammatory M1 and anti-inflammatory M2 macrophages involved a more diverse spectrum of genes and secreted proteins compared with RPE cells. Moreover, the extent of the transcriptomic and secreted cytokine response was superior in macrophages compared to RPE cells. On the other hand, RPE cells expressed particular apoptosis and death receptor genes that might reflect their immunoregulatory role in deviating cellular immune responses, which is important for maintenance of immune privilege of the eye. Thus, our findings suggest that while macrophages appear to engage a plethora of responses, including IFN signaling to control *Mtb* infection and in communication between innate and adaptive immune cells to induce granuloma formation, RPE cells initiate a strong yet incomplete anti-*Mtb* response that primarily depends on IFN signaling to successfully control the early phases of *Mtb* infection in the retina.

The canonical IFN signaling pathway appeared to be the mutual pathway activated in both RPE cells and macrophages, along with IL-6 signaling and the pattern recognition receptors (PRR) pathway involved in bacterial and viral recognition (Supplementary Fig. S1). However, IFN signaling was most strongly activated in *Mtb*-infected RPE cells, with type I IFN (IFNα/β) signaling being dominant over type II (IFNγ) signaling (Figs. 3, 4). This is in line with observations in *Mtb*-infected human pulmonary alveolar epithelial cells.[17–19] Activation of genes associated with IFN signaling in RPE is, however, not specific for *Mtb* infection, as this was also observed upon infection with West Nile virus or vesicular stomatitis virus (VSV, also a single-stranded RNA virus) or upon stimulation with a synthetic analogue (poly I:C) for viral double-stranded RNA.[20–22] Therefore, the observed activation of IFN-inducible genes in *Mtb*-infected RPE cells most likely reflects a general immune response to (intracellular) infection rather than being *Mtb* specific.

IFNs exert both protective and detrimental effects on the host during intracellular bacterial infection. IFNγ is known to induce T-helper (Th)1 responses, and to activate and enhance the expression of antibactericidal molecules in phagocytes to kill intracellular bacteria.[21,23] In RPE cells, both type I and type II IFN are known to inhibit cytomegalovirus (CMV) and *Toxoplasma gondii* replication, which involves indoleamine 2,3 dioxygenase (IDO)-induced tryptophan depletion.[24,25] IDO-1 was also one of the IFN-induced genes we found in *Mtb*-infected RPE. Possibly IDO-induced tryptophan depletion inhibits *Mtb* replication in RPE, but this would require further study.[26] In contrast, excessive IFNα/β signaling has been linked to high *Mtb* disease activity in patients with clinical disease.[18,19] Suppression of cytokines crucial for host defense

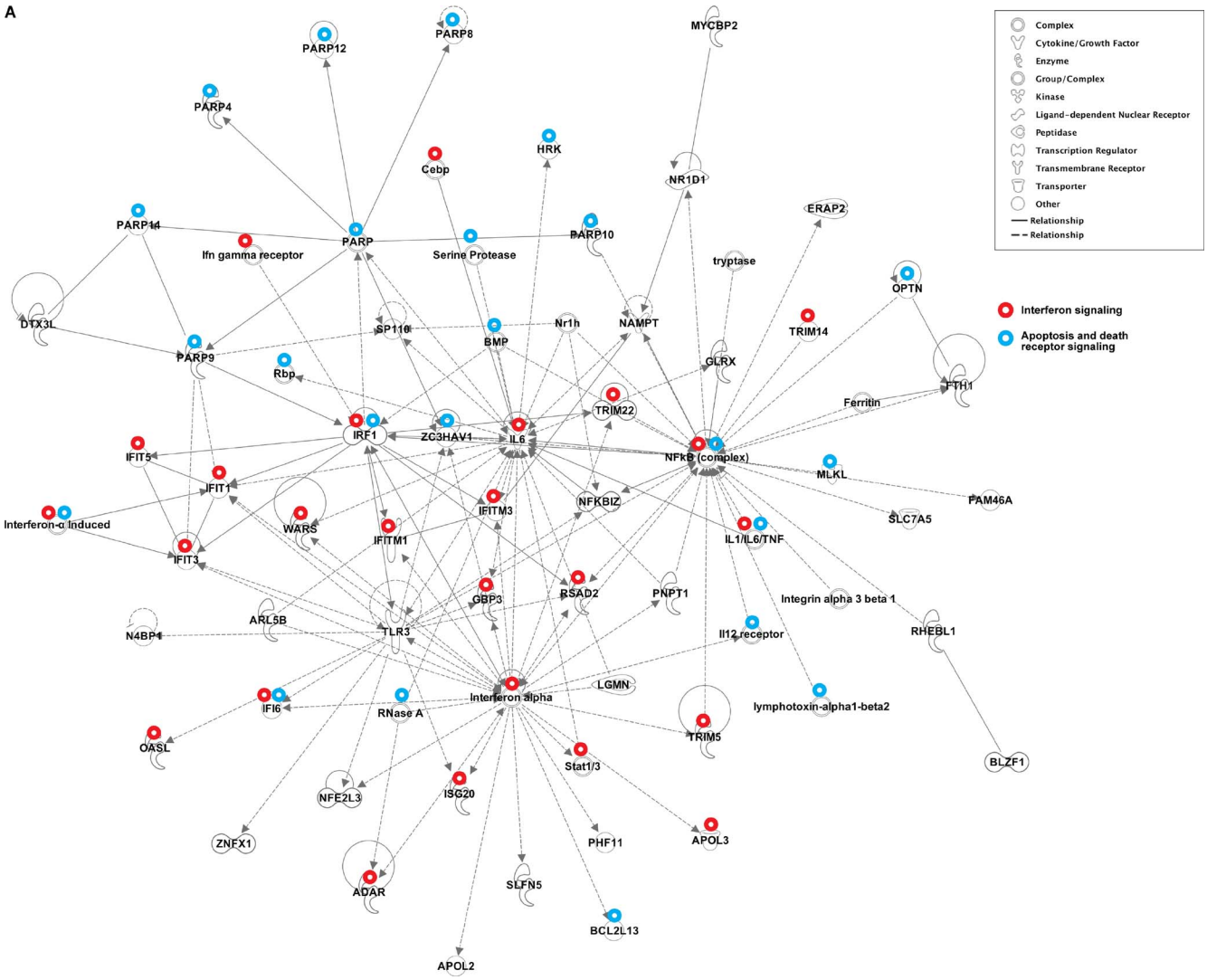

Figure 5. Network analysis of the host response in RPE cells and macrophages following *Mtb* infection. Ingenuity-based pathway analysis of genes that were differentially expressed between (**A**) uninfected and *Mtb*-infected OZR1 cells and (**B**) uninfected and *Mtb*-infected M2 macrophages ($t =$ 24 hours). Shown are the top networks identified in both cell types. Type I and II IFN-inducible genes are highlighted in *red*, apoptosis and death receptor signaling genes are highlighted in *blue*, protein ubiquitination-associated genes are indicated in *green*, and inflammasome-associated genes are shown in *yellow*.

against *Mtb*, including IL-1α, IL-1β, IL-12, and TNFα, and also repression of innate cell responsiveness to IFNγ, have been proposed as important mechanisms of IFNα/β-mediated immunosuppression during *Mtb* infection.[4,20,21,27–31] Moreover, RPE-derived IFNβ can downregulate CXCL9 and intercellular adhesion molecule 1 (ICAM-1) expression by RPE in an autocrine manner. This potentially limits retinal T-lymphocyte/natural killer (NK) cell recruitment and has been proposed as an immunosuppressive mechanism that protects the retina from excessive inflammation, for instance, in the case of RPE infection.[20] Our data suggest that in RPE cells, at least during the early stages of *Mtb* infection, IFN signaling may have a beneficial effect by inhibiting the outgrowth of intracellular *Mtb*. However, it could be speculated that the (prolonged) high induction of IFNα/β could potentially be detrimental at later stages of infection and thereby contributes to *Mtb*-mediated uveitis due to chronic infection or *Mtb* latency in the RPE cells. Clearly, unraveling the exact role or balance of IFN signaling and Th1 induction in RPE in *Mtb*-mediated uveitis requires further investigation.

Molecules related to protein ubiquitination and inflammasome pathways were among the genes more specifically identified in the M2 regulatory network (Fig. 5B). These findings are in line with other in vitro studies demonstrating that *Mtb*-infected macrophages exhibit innate immune functions (including inflammasome activation and ubiquitin-mediated autophagy) to kill intracellular mycobacteria but also to induce adaptive immunity.[3,32] A canonical pathway more prominently regulated in RPE upon *Mtb* infection compared to M2 macrophages was related to cell death and survival (Figs. 3, 5A). One of the apoptosis-related genes that increased in *Mtb*-infected RPE (TNFSF10/TRAIL/APO2L; Supplementary Fig. S2) encodes the proapoptotic membrane expressed molecule TNF-related apoptosis-inducing ligand (TRAIL). TRAIL is expressed by many ocular tissues, including RPE, and contributes to ocular immune privilege, most likely by inducing apoptosis of infiltrating inflammatory cells that

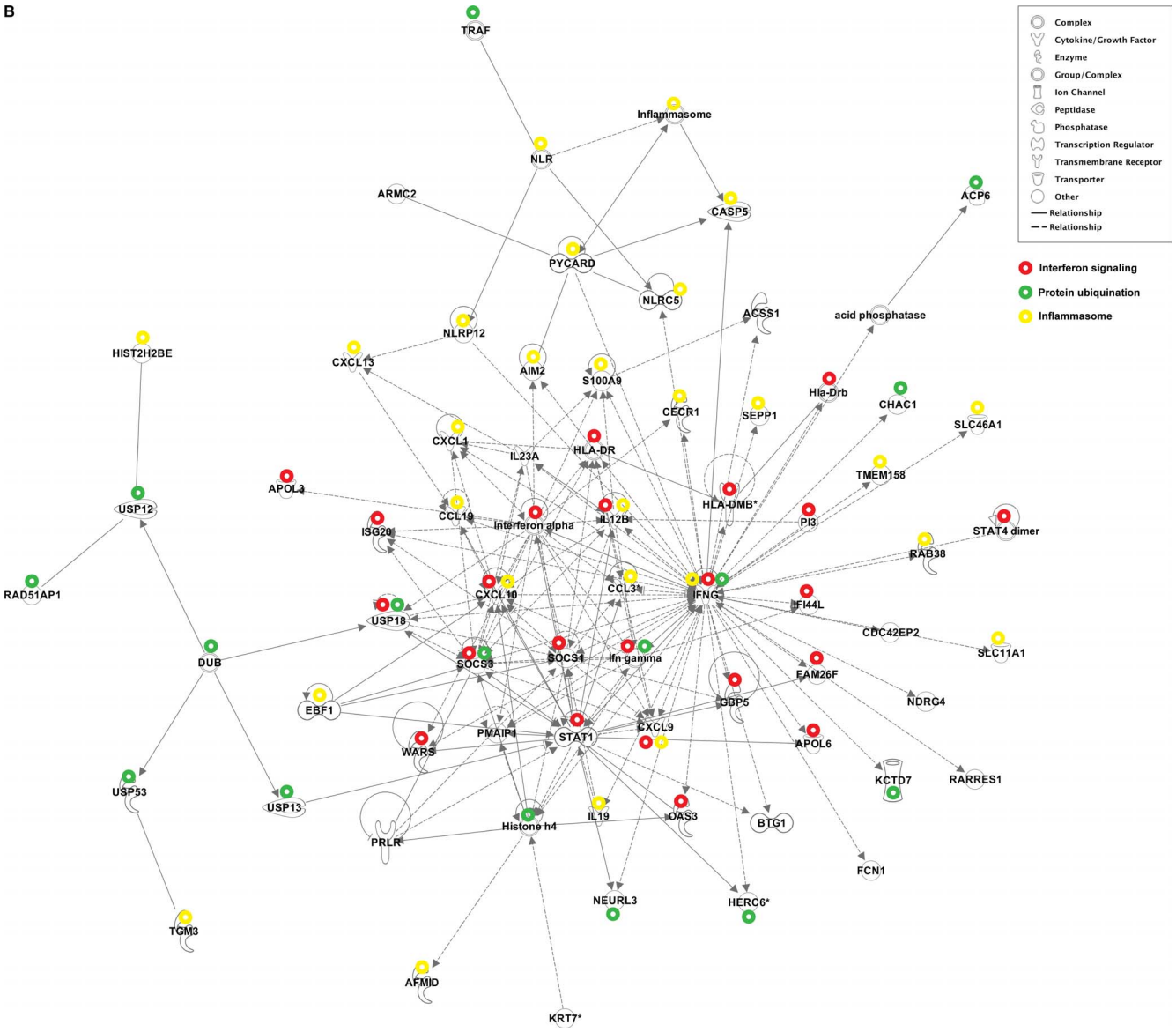

Figure 5. Continued.

express TRAIL-receptor 2 (TRAIL-R2/DR5/TNFRSF10B).[33] Type I IFNs are known to enhance TRAIL expression, for instance on dendritic cells, which enables these cells to induce T-lymphocyte apoptosis.[34] Induction of TRAIL on RPE may thus represent a way to deviate the cellular immune response in order to protect the retina from excessive inflammation and to limit the immunopathologic damage. On the other hand, human RPE cells express TRAIL-R2 (this study and Ref. 33) and necrotic *Mtb*-positive RPE cells have been observed in human eyes,[8] suggesting that TRAIL–TRAIL-R2 interactions between RPE cells may induce death of RPE cells and possibly contribute to inflammation.

RPE cells are well-known producers of mediators that attract and activate different types of leukocytes and as such are considered important initiators/regulators of retinal inflammation.[35,36] Yet *Mtb*-infected RPE secreted substantially lower amounts of cytokines than *Mtb*-infected macrophages did. This might reflect the local ocular function of RPE where only short-distance intercellular communication is required, as opposed to that of macrophages that need to instruct other (immune) cells over longer distances. *Mtb* infection was associated with increased IL-12 production by RPE cells, although it was upregulated to a lesser extent than seen in macrophages. It is tempting to hypothesize that IL-12 derived from *Mtb*-infected RPE cells is involved in local Th1-lymphocyte activation and uveitis-like disease. Also, production of RANTES and IP-10 by *Mtb*-infected RPE cells may further amplify local T-lymphocyte recruitment and activation. This is further supported by observations in a primed mycobacterial uveitis model in rats that was associated with increased production of IP-10.[37] Besides local Th1-lymphocyte activation, it is possible that RPE function in maintaining immune privilege is compromised after a certain degree of infection. *Mtb*-infected RPE cells produced IL-6 that antagonizes TGF-β, which has an important regulatory role in ocular immune privilege.[38] Further insight into the involved pathways may contribute to a better immunopathologic understanding of *Mtb*-associated uveitis, which may also be of benefit for finding new treatment modalities.

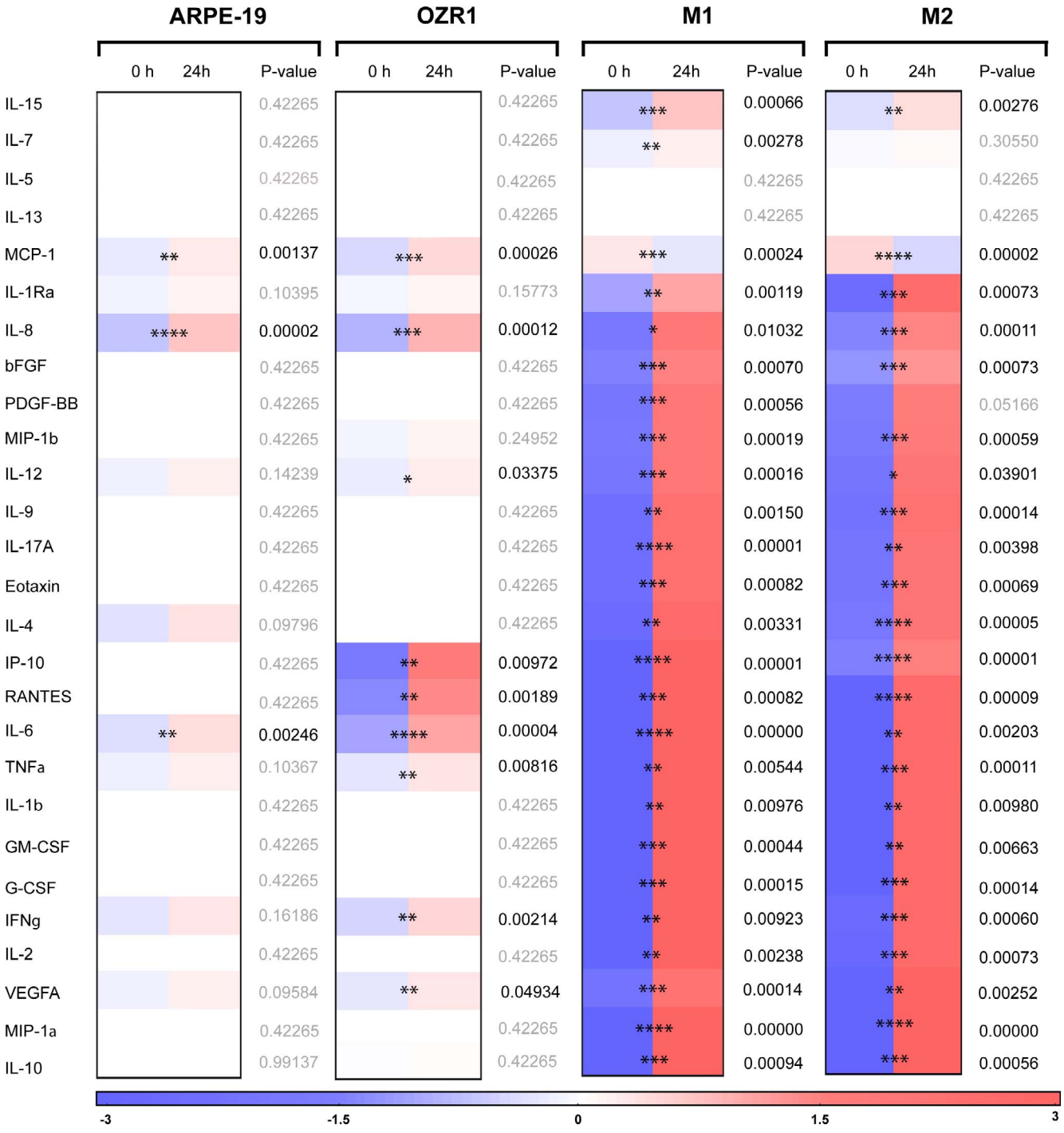

Figure 6. Characterization of the host response at the protein secretion level in RPE cells and macrophages infected with *Mtb*. The heat map is representing changes in cytokine/chemokine/growth factor secretion before and after *Mtb* infection based on the average of triplicate samples. Primary RPE cells OZR1, RPE cell line ARPE-19, proinflammatory M1, and anti-inflammatory M2 macrophages were infected with *Mtb* for 1 hour. Culture supernatants were harvested at 24 hours and analyzed. *Red* indicates increased protein expression levels compared to the geometric mean; *blue* indicates decreased protein expression levels compared to the geometric mean. The color intensity correlates with the magnitude of the calculated fold change. Statistical significance was tested using a Student's *t*-test. $^{*}P < 0.05$, $^{**}P < 0.01$, $^{***}P < 0.001$, $^{****}P < 0.0001$.

In conclusion, we demonstrated that *Mtb* can infect RPE cells and that RPE cells can control the intracellular survival of *Mtb* bacilli similarly to macrophages. However, RPE cells phagocytosed *Mtb* less effectively than macrophages. RPE cells displayed a clear yet restricted anti-*Mtb* response that primarily used IFN signaling to control early phases of *Mtb* infection while macrophages engage a more diverse repertoire of responses including IFN signaling and production of cytokines/chemokines to facilitate communication between innate and adaptive immune cells to induce granuloma formation. RPE cells more strongly activated death receptor and retinoic acid–mediated apoptosis signaling pathways, which are postulated to represent an immunosuppressive mechanism to protect the retina from excessive inflammation and damage.

Investigative Ophthalmology & Visual Science

Acknowledgments

Supported by the Indonesian Ministry of Research Technology and Higher Education and The Netherlands Organization for Health Research and Development (ZonMw-TOP Grant 91214038). The funders had no role in study design, data collection, and analysis; decision to publish; or preparation of the manuscript. Mycobacterial reporter constructs were kindly provided by Jovanka Bestebroer, PhD, Vrije Universiteit Medical Center (VUMC), Amsterdam, The Netherlands.

Disclosure: **R. La Distia Nora**, None; **K.V. Walburg**, None; **P.M. van Hagen**, None; **S.M.A. Swagemakers**, None; **P.J. van der Spek**, None; **E. Quinten**, None; **M. van Velthoven**, None; **T.H.M. Ottenhoff**, None; **W.A. Dik**, None; **M.C. Haks**, None

References

1. World Health Organization. *Global Tuberculosis Report*. Geneva, Switzerland: World Health Organization; 2016.
2. Turner RD, Bothamley GH. Cough and the transmission of tuberculosis. *J Infect Dis*. 2015;211:1367–1372.
3. Watson RO, Manzanillo PS, Cox JS. Extracellular M. tuberculosis DNA targets bacteria for autophagy by activating the host DNA-sensing pathway. *Cell*. 2012;150:803–815.
4. O'Garra A, Redford PS, McNab FW, Bloom CI, Wilkinson RJ, Berry MP. The immune response in tuberculosis. *Annu Rev Immunol*. 2013;31:475–527.
5. Barrios-Payan J, Saqui-Salces M, Jeyanathan M, et al. Extrapulmonary locations of mycobacterium tuberculosis DNA during latent infection. *J Infect Dis*. 2012;206:1194–1205.
6. Randall PJ, Hsu NJ, Quesniaux V, Ryffel B, Jacobs M. Mycobacterium tuberculosis infection of the "non-classical immune cell". *Immunol Cell Biol*. 2015;93:789–795.
7. Wroblewski KJ, Hidayat AA, Neafie RC, Rao NA, Zapor M. Ocular tuberculosis: a clinicopathologic and molecular study. *Ophthalmology*. 2011;118:772–777.
8. Rao NA, Saraswathy S, Smith RE. Tuberculous uveitis: distribution of Mycobacterium tuberculosis in the retinal pigment epithelium. *Arch Ophthalmol*. 2006;124:1777–1779.
9. Nazari H, Karakousis PC, Rao NA. Replication of Mycobacterium tuberculosis in retinal pigment epithelium. *JAMA Ophthalmol*. 2014;132:724–729.
10. Means TK, Wang S, Lien E, Yoshimura A, Golenbock DT, Fenton MJ. Human toll-like receptors mediate cellular activation by Mycobacterium tuberculosis. *J Immunol*. 1999;163:3920–3927.
11. van Bilsen K, van Hagen PM, Bastiaans J, et al. The neonatal Fc receptor is expressed by human retinal pigment epithelial cells and is downregulated by tumour necrosis factor-alpha. *Br J Ophthalmol*. 2011;95:864–868.
12. Verreck FA, de Boer T, Langenberg DM, van der Zanden L, Ottenhoff TH. Phenotypic and functional profiling of human proinflammatory type-1 and anti-inflammatory type-2 macrophages in response to microbial antigens and IFN-gamma- and CD40L-mediated costimulation. *J Leukoc Biol*. 2006;79:285–293.
13. Korbee CJ, Heemskerk MT, Kocev D, et al. Combined chemical genetics and data-driven bioinformatics approach identifies receptor tyrosine kinase inhibitors as host-directed antimicrobials. *Nat Commun*. 2018;9:358.
14. Jett BD, Hatter KL, Huycke MM, Gilmore MS. Simplified agar plate method for quantifying viable bacteria. *Biotechniques*. 1997;23:648–650.
15. Leclerc L, Boudard D, Pourchez J, et al. Quantification of microsized fluorescent particles phagocytosis to a better knowledge of toxicity mechanisms. *Inhal Toxicol*. 2010;22:1091–1100.
16. Joosten SA, Goeman JJ, Sutherland JS, et al. Identification of biomarkers for tuberculosis disease using a novel dual-color RT-MLPA assay. *Genes Immun*. 2012;13:71–82.
17. Mvubu NE, Pillay B, Gamieldien J, Bishai W, Pillay M. Canonical pathways, networks and transcriptional factor regulation by clinical strains of Mycobacterium tuberculosis in pulmonary alveolar epithelial cells. *Tuberculosis*. 2016;97:73–85.
18. Berry MP, Graham CM, McNab FW, et al. An interferon-inducible neutrophil-driven blood transcriptional signature in human tuberculosis. *Nature*. 2010;466:973–977.
19. Ottenhoff TH, Dass RH, Yang N, et al. Genome-wide expression profiling identifies type 1 interferon response pathways in active tuberculosis. *PLoS One*. 2012;7:e45839.
20. Hooks JJ, Nagineni CN, Hooper LC, Hayashi K, Detrick B. IFN-beta provides immuno-protection in the retina by inhibiting ICAM-1 and CXCL9 in retinal pigment epithelial cells. *J Immunol*. 2008;180:3789–3796.
21. McNab F, Mayer-Barber K, Sher A, Wack A, O'Garra A. Type I interferons in infectious disease. *Nat Rev Immunol*. 2015;15:87–103.
22. Munoz-Erazo L, Natoli R, Provis JM, Madigan MC, King NJ. Microarray analysis of gene expression in West Nile virus-infected human retinal pigment epithelium. *Mol Vis*. 2012;18:730–743.
23. Flynn JL, Chan J, Triebold KJ, Dalton DK, Stewart TA, Bloom BR. An essential role for interferon gamma in resistance to Mycobacterium tuberculosis infection. *J Exp Med*. 1993;178:2249–2254.
24. Bodaghi B, Goureau O, Zipeto D, Laurent L, Virelizier JL, Michelson S. Role of IFN-gamma-induced indoleamine 2,3 dioxygenase and inducible nitric oxide synthase in the replication of human cytomegalovirus in retinal pigment epithelial cells. *J Immunol*. 1999;162:957–964.
25. Nagineni CN, Pardhasaradhi K, Martins MC, Detrick B, Hooks JJ. Mechanisms of interferon-induced inhibition of Toxoplasma gondii replication in human retinal pigment epithelial cells. *Infect Immun*. 1996;64:4188–4196.
26. Blumenthal A, Nagalingam G, Huch JH, et al. M. tuberculosis induces potent activation of IDO-1, but this is not essential for the immunological control of infection. *PLoS One*. 2012;7:e37314.
27. de Paus RA, van Wengen A, Schmidt I, et al. Inhibition of the type I immune responses of human monocytes by IFN-alpha and IFN-beta. *Cytokine*. 2013;61:645–655.
28. McNab FW, Ewbank J, Howes A, et al. Type I IFN induces IL-10 production in an IL-27-independent manner and blocks responsiveness to IFN-gamma for production of IL-12 and bacterial killing in Mycobacterium tuberculosis-infected macrophages. *J Immunol*. 2014;193:3600–3612.
29. Teles RM, Graeber TG, Krutzik SR, et al. Type I interferon suppresses type II interferon-triggered human anti-mycobacterial responses. *Science*. 2013;339:1448–1453.
30. Mayer-Barber KD, Andrade BB, Oland SD, et al. Host-directed therapy of tuberculosis based on interleukin-1 and type I interferon crosstalk. *Nature*. 2014;511:99–103.
31. Mayer-Barber KD, Barber DL, Shenderov K, et al. Caspase-1 independent IL-1beta production is critical for host resistance to mycobacterium tuberculosis and does not require TLR signaling in vivo. *J Immunol*. 2010;184:3326–3330.
32. van Crevel R, Ottenhoff TH, van der Meer JW. Innate immunity to Mycobacterium tuberculosis. *Clin Microbiol Rev*. 2002;15:294–309.
33. Hueber A, Aduckathil S, Kociok N, et al. Apoptosis-mediating receptor-ligand systems in human retinal pigment epithelial cells. *Graefes Arch Clin Exp Ophthalmol*. 2002;240:551–556.

34. Leplina OY, Tyrinova TV, Tikhonova MA, Ostanin AA, Chernykh ER. Interferon alpha induces generation of semi-mature dendritic cells with high pro-inflammatory and cytotoxic potential. *Cytokine*. 2015;71:1–7.
35. Bastiaans J, van Meurs JC, van Holten-Neelen C, et al. Factor Xa and thrombin stimulate proinflammatory and profibrotic mediator production by retinal pigment epithelial cells: a role in vitreoretinal disorders? *Graefes Arch Clin Exp Ophthalmol*. 2013;251:1723–1733.
36. Holtkamp GM, Kijlstra A, Peek R, de Vos AF. Retinal pigment epithelium-immune system interactions: cytokine production and cytokine-induced changes. *Prog Retin Eye Res*. 2001;20:29–48.
37. Pepple KL, Rotkis L, Van Grol J, et al. Primed mycobacterial uveitis (PMU): histologic and cytokine characterization of a model of uveitis in rats. *Invest Ophthalmol Vis Sci*. 2015;56:8438–8448.
38. Ohta K, Yamagami S, Taylor AW, Streilein JW. IL-6 antagonizes TGF-beta and abolishes immune privilege in eyes with endotoxin-induced uveitis. *Invest Ophthalmol Vis Sci*. 2000;41:2591–2599.

Investigative Ophthalmology & Visual Science